

**NUREG/CR-3242  
LA-9929-MS**

**RI**

# **The Los Alamos National Laboratory/ New Mexico State University Filter Plugging Test Facility**

## **Description and Preliminary Test Results**

D. L. Fenton\*  
J. J. Dallman\*  
P. R. Smith\*  
R. A. Martin  
W. S. Gregory

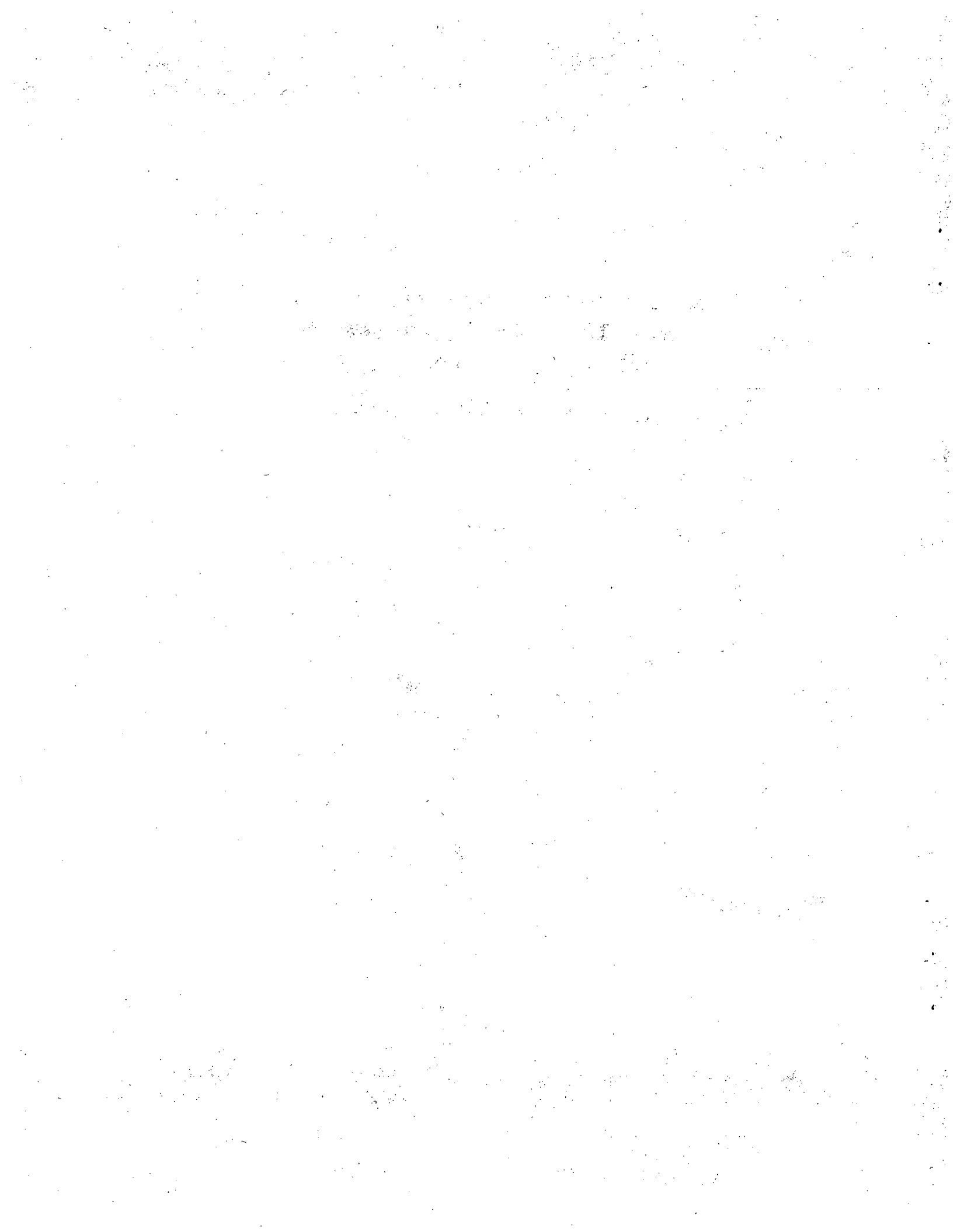
Manuscript submitted: October 1983  
Date published: October 1983

Prepared for  
Division of Risk Analysis  
Office of Nuclear Regulatory Research  
US Nuclear Regulatory Commission  
Washington, DC 20555

NRC FIN No. A7029

\*Mechanical Engineering Department, New Mexico State University, Las Cruces, NM 88003.

**Los Alamos** Los Alamos National Laboratory  
Los Alamos, New Mexico 87545



THE LOS ALAMOS NATIONAL LABORATORY/NEW MEXICO STATE UNIVERSITY

FILTER PLUGGING TEST FACILITY

Description and Preliminary Test Results

by

D. L. Fenton, J. J. Dallman, P. R. Smith,  
R. A. Martin, and W. S. Gregory

ABSTRACT

A facility to test the plugging effects of combustion products on high-efficiency particulate air filters has been constructed. This facility can supply experimental data to support pressure-drop models of filter plugging under fire accident conditions, which are needed for use in an existing fire accident analysis computer code. The test facility includes a specially designed null-balance filter-weighing system. The resolution of this system is approximately 2 to 3 g out of 14 kg for a commercial 0.6- by 0.6-m filter. Using this system, commercial filters can be tested to provide data with which to correlate pressure drop and smoke aerosol mass accumulation and flow rate. Some recently accomplished tests and future test plans are discussed.

---

I. INTRODUCTION

A. Background

Most nuclear facilities depend on ventilation systems to bring air into, through, and out of them. Because the air passes through contaminated areas,

most ventilation systems contain air cleaning systems of which the high-efficiency particulate air (HEPA) filter is an important component. A standard HEPA filter consists of pleated filter material enclosed by a plywood or metal frame. The filter material (which is made up of a thin mat of fine, intertwined glass fibers) is folded back and forth around thin sheets of asbestos or aluminum, which are called separators. The nominal airflow capacity of these filters is  $0.47 \text{ m}^3/\text{s}$ .

An air cleaning system may consist either of a series arrangement of these filters or of banks containing several hundred filters. HEPA filters typically exhibit cleaning efficiencies of 99.97% or better, and operate very effectively in most noncorrosive atmospheres at normal airflow conditions. However, there is concern about the degradation of performance or destruction of these units when they are subjected to accident conditions. The areas of concern are (1) the structural integrity of the HEPA filter media, (2) the influence of design and construction on structural integrity, (3) the filtration effectiveness, and (4) the plugging or clogging of the media by combustion products.<sup>1</sup> This report deals with area (4).

HEPA filters may be exposed to large quantities of smoke (solid and liquid aerosol) under fire accident conditions. If the filters become sufficiently plugged, upstream safety zones that previously were maintained at negative gauge pressures (slight vacuums) could assume positive gauge pressures and leak radioactive aerosols.<sup>2</sup>

## B. Purpose

The Los Alamos National Laboratory filter plugging program is part of a more comprehensive accident analysis effort sponsored by the US Nuclear Regulatory Commission.<sup>3</sup> The filter plugging experiment program was begun in 1981, which is when we realized that there were no known data for simultaneous measurements of pressure drop, flow rate, and combustion product mass accumulation on HEPA filters for realistic fire conditions. These data are needed to calculate the empirical coefficients used in expressions relating filter pressure drop to volumetric flow rate in the Los Alamos FIRAC accident analysis computer code.<sup>4</sup> An example of a typical semi-empirical expression of this kind is<sup>5</sup>

$$\Delta p = \Delta p_0 (1 + \alpha m_p) \quad , \quad (1)$$

where

$$\Delta p_0 = K_L \mu \frac{Q}{A^{3/2}} + K_T \rho \frac{Q^2}{A^2} \quad (2)$$

Equation (1) assumes that a linear relationship exists between  $\Delta p/Q$  and  $m_p$ . In Eqs. (1) and (2),  $\Delta p_0$  represents the clean filter pressure drop resulting from both laminar friction and turbulent dissipation in pascals, and

$\alpha$  = filter plugging coefficient dependent on filter and material properties ( $\text{kg}^{-1}$ ),

$m_p$  = accumulated mass of material on filter (kg),

$Q$  = volumetric flow rate ( $\text{m}^3/\text{s}$ ), which =  $VA$ ,

$Q_0$  = clean filter volumetric flow rate, which =  $V_0 A$ ,

$V$  = velocity (m/s),

$A$  = filter cross-sectional flow area ( $\text{m}^2$ ),

$K_L, K_T$  = dimensionless laminar and turbulent coefficients, respectively,

$\mu$  = air dynamic viscosity ( $\text{Pa}\cdot\text{s}$ ), and

$\rho$  = air density ( $\text{kg}/\text{m}^3$ ).

Other more complicated theoretical models of filter plugging are available in the literature, such as the dendrite and increasing fiber models.<sup>6</sup> The models quantitatively predict filter plugging as idealized cases in which the loading particles either form fiber-like dendrite chains or increase the fiber diameter, respectively. (In actuality, both effects probably are occurring in the case of smoke.) These models are extensions of existing pressure drop theories for clean filters. A computer code that simulates smoke movement through a facility must have the capability to alter the flow dynamics in accordance with material accumulation on the filter. The FIRAC computer code is capable of predicting temperature and smoke distributions throughout a nuclear facility ventilation system. The data developed in this program will be transformed into filter plugging relationships for the FIRAC code, which automatically will adjust

the flow conditions in accordance with the mass of material on the filter. This simulation capability is essential if an analyst is to predict flow reversals and the effect of the changing ventilation conditions on the character of the fire. That is, reduced airflow may create greater smoke production and flow reversals that will send backflow to less contaminated zones within the plant. Therefore, the purpose of the Los Alamos filter plugging program is to supply experimental data to support the generalized pressure drop model:

$$\Delta p / \Delta p_0 = f(m_p) (Q/Q_0) \quad (3)$$

This expression relates the filter plugging variables

1. pressure drop,
2. volumetric flow rate, and
3. mass accumulation

in a systematic way. The form of the polynomial  $F$  in Eq. (3) and some empirical coefficients will depend on other important filter plugging variables, including

4. aerosol type/chemistry,
5. aerosol concentration,
6. aerosol size distribution,
7. water vapor,
8. air temperature, and
9. other things (such as electrostatic effects, flow conditions, and filter media parameters).

Some theoretical aspects of filter plugging are discussed in Refs. 7--9.

### C. Scope

The current filter plugging test series is part of a Los Alamos fire test plan to support the development and verification of the FIRAC computer code. Ultimately, we wish to model and predict transient combustion product generation and transport in nuclear fuel cycle facilities using FIRAC. To do this, we need to develop experimental fire simulation and measurement capabilities in the following areas.

1. Fire simulation and classification
2. Compartment fire behavior

3. Combustion product behavior during transport (deposition and modification by aerosol dynamic changes)
4. Filter plugging behavior
5. FIRAC code verification

The testing in these areas should include release rate oven, compartment fire, filter plugging, and ventilation system facility experiments.

To supply the needed filter plugging data, Los Alamos and New Mexico State University (NMSU) have constructed a unique filter plugging test facility. Its purpose is to supply experimental data for 0.61- by 0.61-m HEPA filters under conditions simulating those postulated as credible for fires in nuclear facilities. Industrial fires such as these are expected to differ from other kinds of fires in the types of materials involved and the ventilation conditions (availability of oxygen). A typical fuel mixture may be composed of the materials listed in Table I. These materials are likely to burn under both oxygen-rich and oxygen-starved conditions (over- and under-ventilated conditions) to produce particulate material, water vapor, and gaseous combustion products. Thus, some unique capabilities were required of the new facility.

First, we needed the capability to determine the accumulated mass gain of a clean 14-kg HEPA filter because of smoke and moisture clogging. Previous tests using polystyrene latex spheres led us to expect plugging (arbitrarily defined to be a 50% reduction in flow rate from the design value) to occur from an accumulation of under 500 g of dry solid material. To resolve 2- to 3-g smoke accumulations out of 14 kg, we designed and constructed a special null-balance filter-weighing apparatus. Second, we needed the capability to burn mixtures of

TABLE I

TYPICAL FUEL MIXTURE COMPOSITION

<u>Component</u>	<u>Composition (%)</u>
1. Polymethylmethacrylate	45
2. Cellulosic	26
3. Elastomer	18
4. Polyvinyl Chloride	8
5. Hydraulic Fluids	2
6. Polystyrene	1

materials selected from Table I that have variable burning efficiencies. To do this, Battelle Pacific Northwest Laboratory (PNL) designed and constructed a special combustor for Los Alamos. Lastly, we needed the capability of adding varying amounts of heat and moisture to the airflow. Heat was supplied by a commercial air heater, and water was sprayed into the air through a commercially available nozzle.

This report describes the construction and preliminary check-out of the filter plugging facility. Full-size HEPA filters initially operating at their design pressure drop and flow rate of approximately 2.54 cm w.g. and 0.47 m<sup>3</sup>/s, respectively, were selected for testing to ensure realistic results and to eliminate the uncertainty of scaling. (HEPA filters are operated under these same conditions in nuclear facilities.) However, a special problem resulted from this experimental approach. Because the mass of a clean HEPA filter is on the order of 14 kg, how could the accumulated particulate mass (on the order of 100 g) be measured reliably? Several design options were considered, but we finally decided on a null technique. This technique incorporates a carefully designed balance and counterweights so that the initial weight of the HEPA filter can be cancelled or nulled. During tests when the HEPA filter is being loaded with particles, the imbalance is measured directly by means of a sensitive force transducer. We achieved the desired mass resolution (2 to 3 g) with the balance.

Real-time measurement of HEPA filter mass gains was determined to be too difficult to accomplish at the present time. This would require the HEPA filter to be suspended permanently on the force transducer in such a way as to subtract—mechanically or electrically—the aerodynamic forces applied by the flow through the filter. Instead, the flow is diverted from the filter (or stopped), and it is unclamped from its loading position for the mass-gain measurement.

The design details of the equipment and some preliminary test results are described in Sec. II. These results must be considered tentative because they involve the initial operation of all the equipment. For these tests, we used a commercial high-volume particle generator to create a stearic acid aerosol. Stearic acid produces a submicron-size aerosol and is safe for human contact.



## II. HEPA FILTER PARTICULATE LOADING EQUIPMENT

The HEPA filter being tested was attached to the mass balance and the surrounding ductwork. The ducts upstream from the test filter bring air and the test aerosol to the filter; downstream ducts conduct air from the filter and provide the means for measuring both the pressure drop across the filter and the actual volumetric airflow rate through the filter. A special branch is located upstream from the filter to divert the test aerosol from the test filter during weighing. The equipment and instrumentation are as follows.

1. 3465A Digital Multimeter  
Hewlett Packard, Colorado Springs, Colorado
2. 6271A DC Power Supply  
Harrison Laboratories, Berkeley Heights, New Jersey
3. No. TD-6-1K Force Transducer  
Schaevitz Engineering, Camden, New Jersey
4. 700-1A Soni-Mist Nozzle  
Heat Systems Ultrasonics, Plain View, New York
5. Model 258 Smoke Generator  
Hiac/Royco Instruments, Menlo Park, California
6. Model 351 Toggle Clamps  
De-Sta-Co, Detroit, Michigan
7. Two Manometers (one inclined and one vertical)  
Dwyer Instruments, Michigan City, Indiana
8. Pneumatic Cylinders  
Miller Fluid Power, Bensenville, Illinois
9. Psychrometer  
Dwyer Instruments, Michigan City, Indiana
10. Axial Flow Fan  
Joy Manufacturing, Chicago, Illinois

### A. Air-handling Equipment, Smoke Generator, and Water Spray Nozzle

The air-handling equipment is composed of a fan housed within a box and both wood and metal ducts. The maximum capacity of airflow through the system is approximately  $34 \text{ m}^3/\text{min}$ . The wooden ducts are made of 1.9-cm-thick plywood and are reinforced with 5.1- by 5.1- by .63-cm angle iron; they were constructed at the NMSU Mechanical Engineering Machine Shop. The metal ducts are made of

heavy-gauge galvanized sheet metal and are reinforced with angle iron; they were fabricated by a local refrigeration contractor. The sheet-metal ducts constitute the three main sections of the air ductwork: (1) the diverging transition section; (2) the by-pass and by-pass exit ducts; and (3) the converging, transition, and exit ducts. The center of all the ductwork is 1.08 m above the ground, which allows the assembly process to proceed more quickly than if the ducts were on the ground. The ductwork for the most part measures 0.61 m by 0.61 m. Figures 1 and 2 show the major components of the system. The ductwork and the test filter instrumentation are shown in Figs. 3 and 4, respectively.

The fan or air blower is an axial vane fan made by Joy Manufacturing. It is rated at  $68 \text{ m}^3/\text{min}$  and is powered by a 5.7-kW Dyna Corporation motor operating at 1720 rpm. The fan is mounted in a wooden box with an adjustable inlet that allows the airflow rate to be varied. The air is cleaned initially by a furnace filter at the inlet, which extends the operating life of the pre-filter. To reduce fan losses, a bleed-off branch downstream from the box has a damper and returns air to the fan box.

The fan box exit is 0.3- by 0.3-m square and includes a vibration isolation device that connects the fan box to the duct. The vibrations of the fan motor are damped by the isolation device, which is 15.24 cm long and made of a

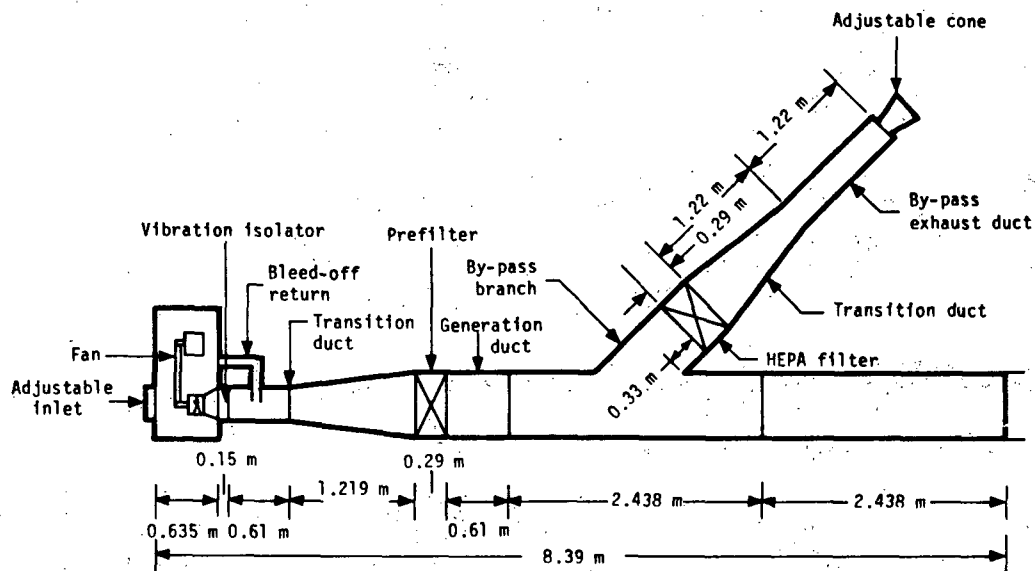


Fig. 1.  
Wind tunnel system—upstream section (top view).

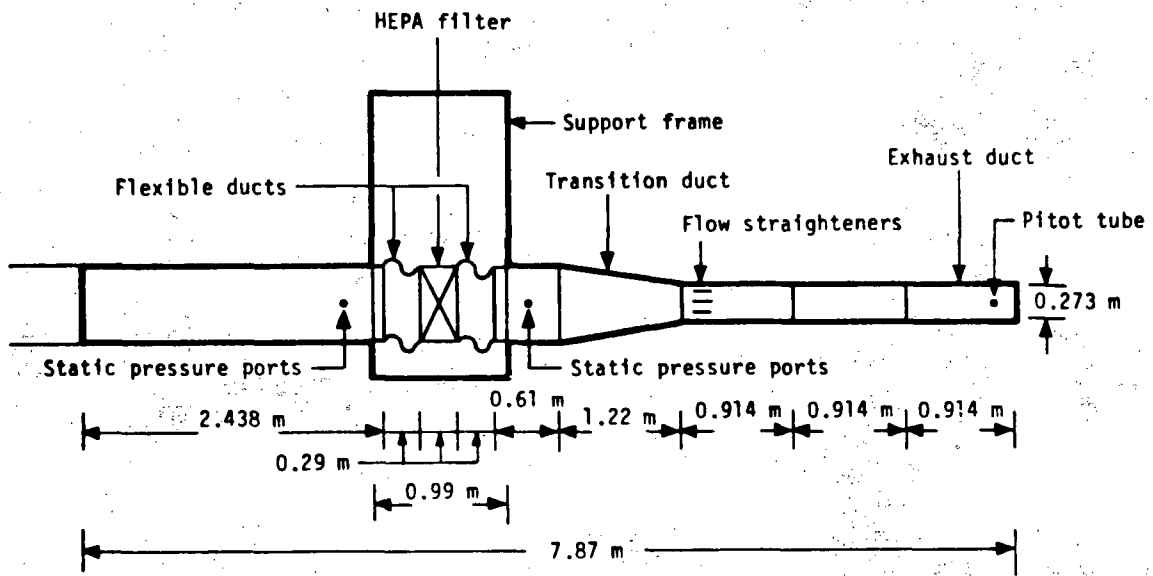


Fig. 2.  
Test facility duct work.

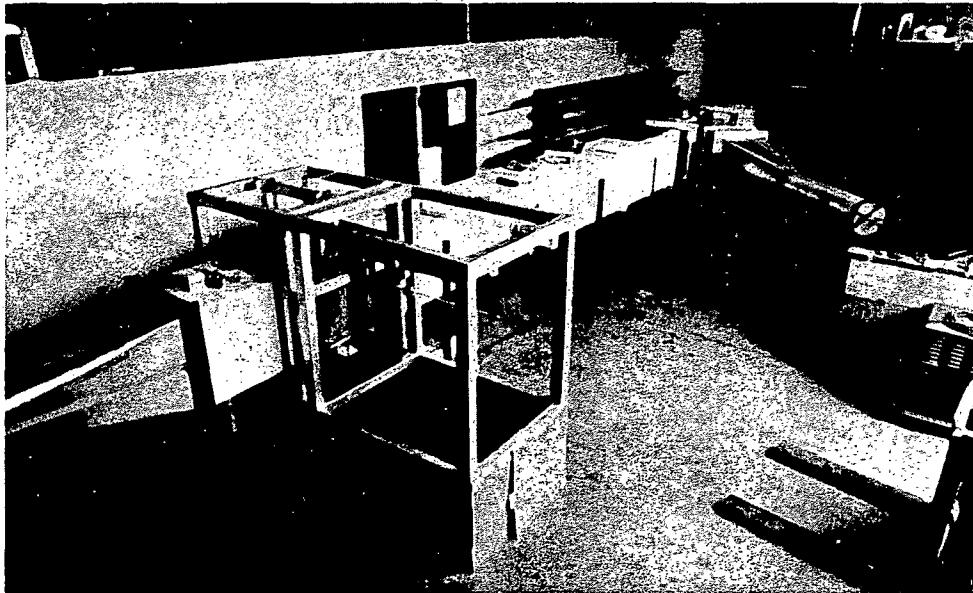


Fig. 3.  
Test filter instrumentation.

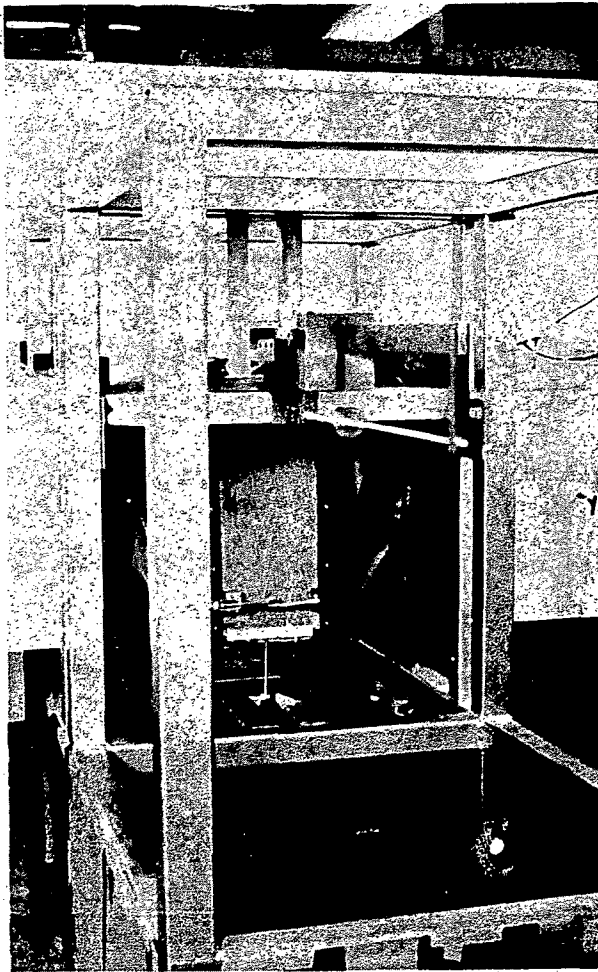


Fig. 4.  
Test filter instrumentation.

flexible, strong fabric that commonly is used by the ventilation industry. The vibration isolator is connected to a 0.3- by 0.3- by 0.61-m sheet-metal duct. The airflow is made to expand or diverge smoothly to a 0.61- by 0.61-m duct size. This is to accommodate the HEPA filter size used in testing. The expansion is accomplished by a 1.2-m-long sheet-metal transition duct in which the wall angle from the horizontal centerline is not greater than  $7^{\circ}$ .

The prefilter collects particles greater than 1 or 2  $\mu\text{m}$ , lint, and dust concentrations greater than  $22.9 \text{ mg/m}^3$  as established in Ref. 1. In the nuclear power industry, the main purpose of the prefilter is to prolong the life of the HEPA filter, whereas at the NMSU facility the purpose is to create a clean airstream into which the generated particles can be injected (Fig. 1). The prefilter also acts as a flow straightener, destroying the large flow features created by the fan and transition duct.

The generation duct is a 0.61- by 0.61- by 0.61-m section with two ports (for particle and water spray injections); Fig. 5 shows the arrangement of these injection ports. The smoke or aerosol is produced by a Royco Model 258 smoke generator (shown schematically in Fig. 5). The smoke generator is essentially a commercial pressure cooker with six special nozzles placed in the lid. The jet nozzles are immersed in a liquid mixture of alcohol and stearic acid. Each nozzle produces 85 L/min. The generator has an output mass concentration of 5 mg/L with a median particle diameter of 0.3  $\mu\text{m}$ . (These generator performance specifications are for the smoke material, dioctyl phthalate or DOP,<sup>10</sup> which was not used in the filter tests discussed here.)

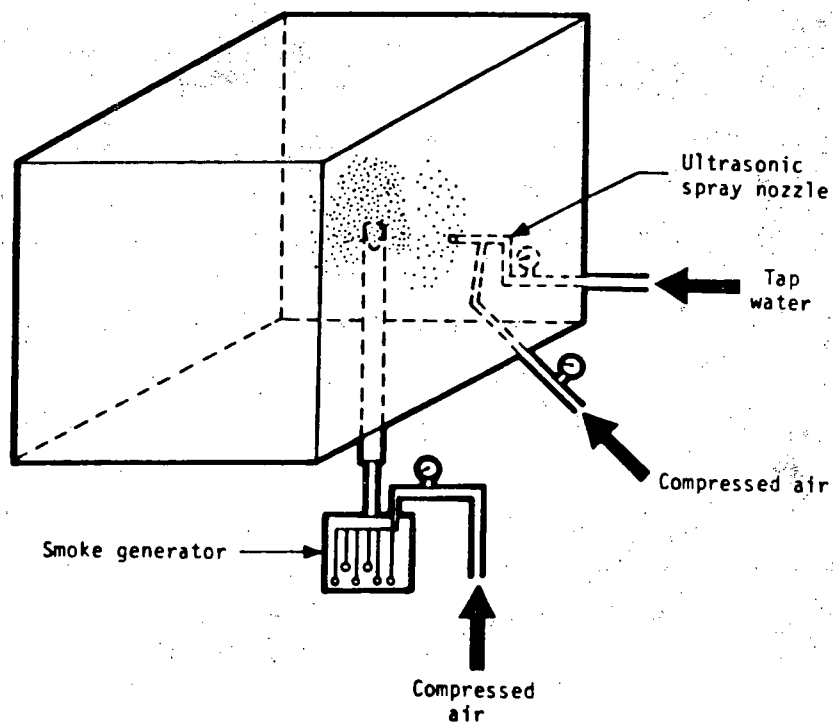


Fig. 5.  
Generation duct.

A significant portion of the first experimental HEPA filter loading tests involved water mist injection to determine the importance of this variable.<sup>1</sup> Water vapor concentrations were selected to bracket those expected by combustion. The water mist was produced by a Soni-Mist Ultrasonic Spray Nozzle (Model 700-1A), which is capable of producing  $0.21 \text{ m}^3/\text{min}$  at 414 kPa. The exact size of the water spray droplets is unknown, but they are believed to be initially in the size range of 5--15  $\mu\text{m}$ .

The diverting or by-pass duct allows the operator to pass the flow from the test branch to a similar branch by means of sliding sheet-metal panels as shown in Fig. 1. Each panel slides in across the duct to block the flow, but only one panel is used at a time (depending on which test condition exists). Either the filter is being loaded with particles (the by-pass branch is blocked), or the filter is being weighed (the test branch is blocked). This procedure can be used to ensure consistent flow conditions (constant air velocity and constant particle and water droplet concentrations).

The by-pass duct is made of sheet metal and diverges from the test branch at an angle of  $45^\circ$ . The by-pass branch is 0.61- by 0.61-m square and leads to a

HEPA filter, which is followed by a converging transition duct and exit. A movable cone at the exit provides adjustable regulation of the flow. Figure 1 gives the overall dimensions of the by-pass duct.

After passing through the test filter, the airstream proceeds through a 0.61- by 0.61- by 0.61-m wooden duct into a converging sheet-metal transition duct. The transition duct changes gradually from the 0.61- by 0.61-m square to a cylindrical duct 0.273 m in diameter. There is a series of three 0.91-m-long cylindrical ducts, resulting in a total length of 2.74 m. The exhaust is at the end of the third duct, which also contains a pitot tube for measuring the centerline velocity pressure. An inclined Dwyer manometer (read in centimeters water gauge) gives the velocity pressure. Flow straighteners are placed a distance of five duct diameters upstream of the pitot tube to prevent flow swirl. The resolution of the manometer is about 0.005 cm w.g. Because the relation between velocity pressure and velocity is nonlinear, the velocity resolution is approximately 0.1 m/s.

## B. Test Section

The test section of the system is at the HEPA filter being tested. The test filter is about 4.8 m, or about eight duct diameters, from the branch ductwork. The instrumentation at the test section includes a mass balance, a force transducer, and a vertical manometer to measure static pressure drop across the filter.

1. Filter Weighing System. The balance beam assembly is designed to null the starting filter weight. The filter is attached to one end of the beam and can be balanced on the other side by moving adjustable counterweights.

The balance is delicate and is protected from vibration and outside forces (including people) by a large support structure. The structure is made of 7.62-cm-square steel tubing with a wall thickness of 0.317 cm. The tubing is welded together into the frame shown in Figs. 6 and 7. The frame is 1.77 m high, 0.9906 m wide, and 2.24 m long. It is leveled using adjustable legs. The beam (shown in Figs. 6 and 8) is 1.27 cm thick, 5.1 cm wide, and 160.3 cm long. It is held rigid by a cradle that balances on a knife-edge. All the components of the balance beam are made from mild steel to facilitate the machining of the knife-edge and cradle angles.

A knife-edge support assembly was selected for the balance beam because of its inherent simplicity. The alternative support assemblies that we considered

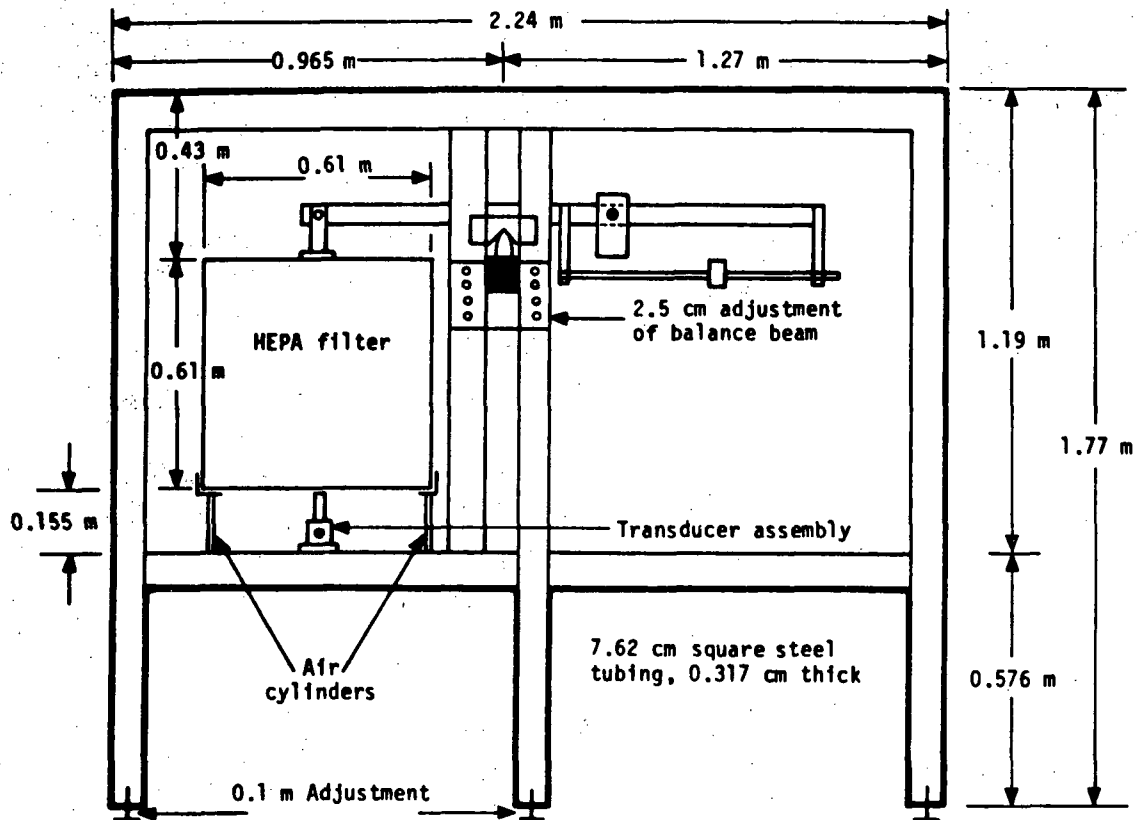


Fig. 6.  
Balance beam assembly and support structure (front view).

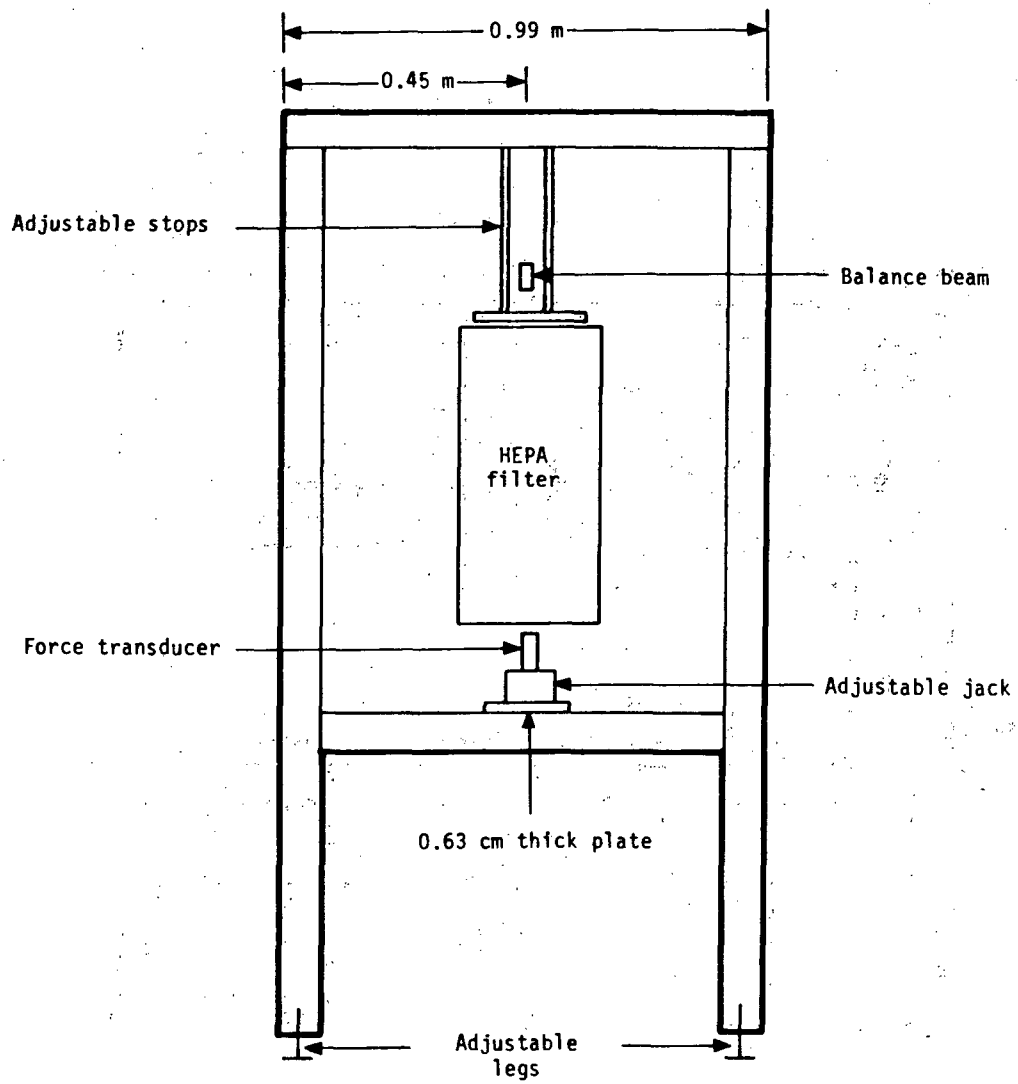


Fig. 7.  
Balance beam assembly and support structure (side view).



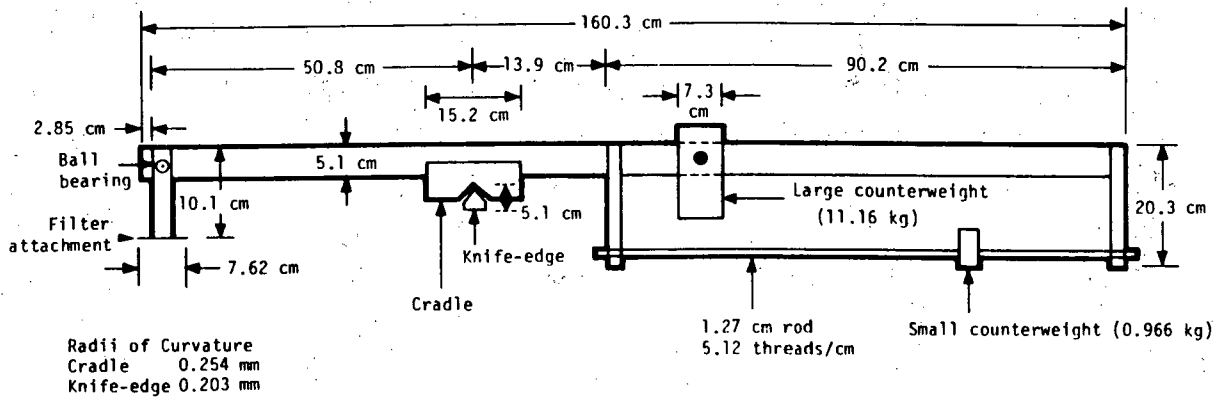


Fig. 8.  
Balance beam assembly.

required significantly more construction effort and additional utilities (such as clean compressed air) for low-friction operation. Faries gives an analysis of the contact stresses involved that indicates that the maximum shearing stress is generally the most important one because this stress is responsible for promoting flaking of metal particles from the surface.<sup>11</sup> With these considerations and assuming a safety factor of 4, the knife-edge radius of curvature was calculated as 0.203 mm for mild steel and a length of 10 cm. To achieve the desired stress distribution, the cradle, which fits atop the knife-edge, had to have a radius of curvature of 0.254 mm.

The knife-edge component is a solid five-sided polygon 5.1 cm high and 10.1 cm long. (The exact dimensions are 3.8 by 1.9 by 3.8 by 3.8 by 1.9 cm.) Figure 8 shows the knife-edge and the general location of the beam. The cradle is 6.52 cm thick, 15.2 cm wide, and 10.1 cm deep. Both the knife and cradle were inspected under a microscope to ensure that the design values were obtained.

The large counterweight mass is 11.16 kg. It can be adjusted by sliding it along the beam and is secured with a thumbscrew. The small counterweight mass is 0.966 kg. It is adjusted by turning the weight on a 2.27-cm threaded rod; two 1.26-cm nuts lock the weight after the initial balance has been achieved. The small mass can produce a resolution of 3.71 g per turn. Figure 8 shows the dimensions of the counterweights. The maximum and minimum filter weights that can be nulled are 29.3 kg and 5.86 kg, respectively.

The filter is attached to the beam by a cradle-and-bearing arrangement (Fig. 8). High-precision, self-aligning ball bearings prevent the filter from

binding or sticking. This is important for the operation of the force transducer and is discussed later. Air cylinders and adjustable stops hold the test filter stationary to protect the knife-edge from the destructive horizontal forces that occur during the particle loading mode. The filter also must be able to hang freely when a mass measurement is to be taken. Two double-acting air cylinders fulfill both of these requirements and allow quick conversion from one mode to the other. The air cylinders are capable of a 15.2-cm stroke of which 13.6 cm is used in the actual system. The filter is stopped at a height equal to that of the duct by an iron frame or adjustable stop that is connected to the support frame. Figures 6 and 7 show the exact positioning of the cylinders and stop.

The particle mass collected by the filter is measured by a force transducer. The transducer has a range from 0 to 1000 g and has a reported linearity error of 0.6 over the full range. The transducer operates at 15 V, which is supplied by a direct current power supply. The transducer reads out on a digital multimeter.

Two 7.62-cm-square steel tubing cross beams located underneath the test filter support the transducer assembly. The assembly includes (1) a 0.63-cm-thick plate, (2) a Micro-Control jack with a 5.1-cm throw, and (3) the force transducer. The force transducer is bolted to the jack, which is bolted to the plate, and the plate is bolted to the cross beams. The separation distance between the filter bottom and the transducer platform is 0.64 cm. The descent of the filter onto the transducer is controlled to some extent by the high-precision ball bearings in the filter attachment. The bearings allow the filter to consistently hang and swing free so that the bottom of the filter remains parallel to the horizontal and forms a  $90^{\circ}$  angle with the transducer platform.

The calibration curve of the force transducer is shown in Fig. 9. The points were taken after the filter weight had been nulled. Known values of mass were placed on top of the filter, and the transducer reading was recorded. A third-degree polynomial curve-fit yields the following equation.

$$M = 4.39 \times 10^{-8} V^3 - 3.24 \times 10^{-4} V^2 + 0.932 V - 13.48 ,$$

where  $V$  is the transducer output voltage measured in millivolts and  $M$  is the mass in grams. Note that the actual linearity of the transducer/mass balance combination is 11% of span.

2. Flexible Ducts. The flexible ducts shown in Fig. 10 allow the separation of the test filter from the duct system when making a mass measurement or filter change. Eight quick-release latches bolted to the filter flange of the flexible ducts enable the separation to proceed quickly. The two ducts measure .61 by .61 by .28 m, and the flexible material is the same material used in the vibration isolation device.

3. Test Filter Static Pressure Drop. The static pressure drop across the filter is measured in centimeters water gauge by a Dwyer vertical manometer with

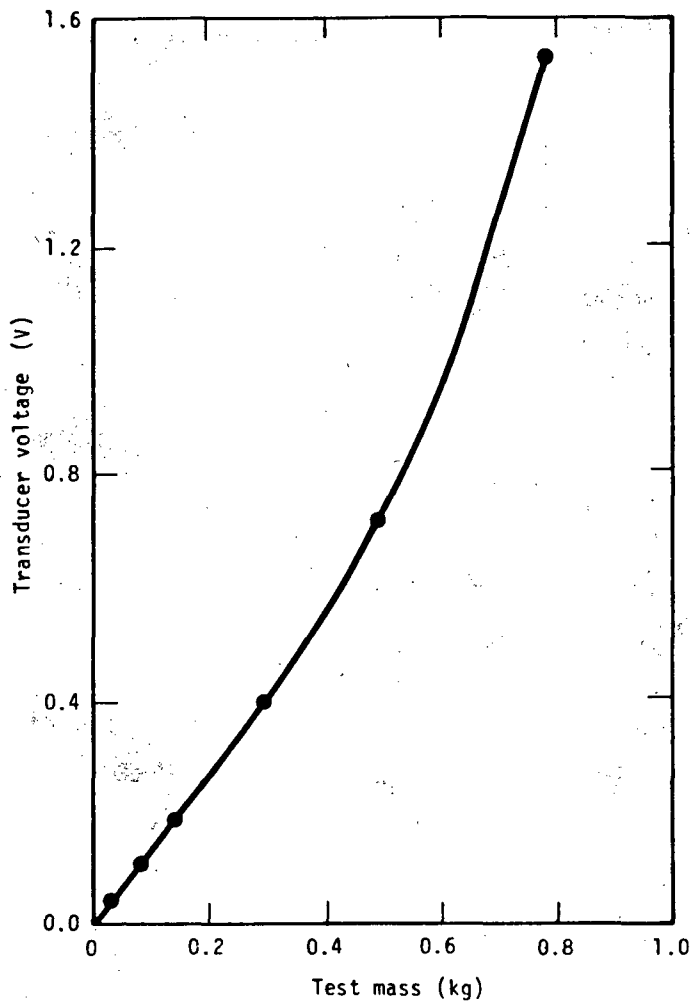


Fig. 9.  
Transducer calibration.

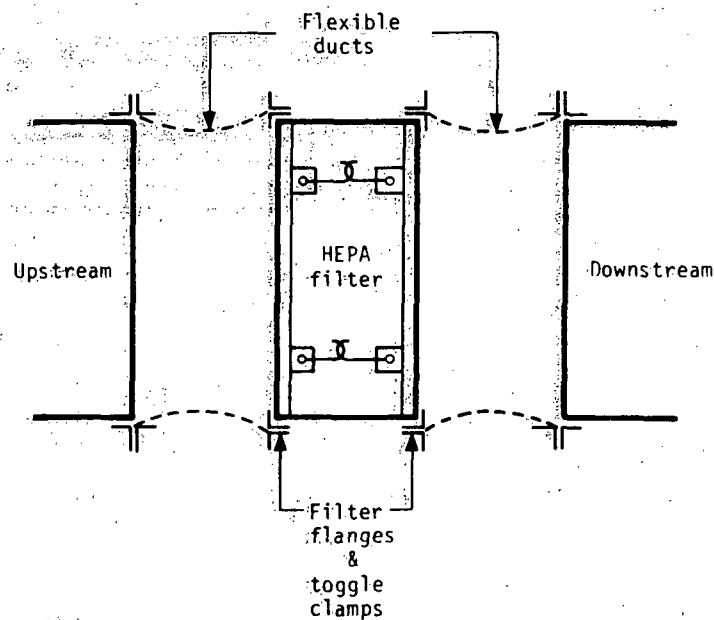


Fig. 10.  
Test filter section.

a resolution of 1 mm. The upstream and downstream static ports are placed 0.45 m from their respective filter faces. The large distance is a result of the length of the flexible ducts.

### III. PRELIMINARY HEPA FILTER PLUGGING TESTS

A preliminary series of 19 idealized plugging tests was conducted during the winter of 1981 (1) to test the null-balance filter-weighing system and (2) to determine the effects of concentration and moisture addition.<sup>1,12</sup> In these tests, dry stearic acid particles with a mean diameter of 0.488  $\mu\text{m}$  were generated using a commercial condensation-type generator. Stearic acid was chosen because a fairly monodisperse, spherical, nontoxic, control aerosol could be generated for the approximate size desired to simulate a fire. (We were only able to generate stearic acid aerosol loadings of about 60 to 120  $\text{mg}/\text{m}^3$ ; full-scale forced-ventilation fire tests at the Lawrence Livermore National Laboratory have produced concentrations of real smoke in excess of 5  $\text{g}/\text{m}^3$  while burning porous cribs of solid fuels.) A spray nozzle was used to inject water at selected flow rates up to fully saturated conditions.

Nineteen tests (including dry particulate only, water only, and mixed conditions) were conducted. In these tests, the filter volumetric flow rate initially was set at 28.3 m<sup>3</sup>/min and then allowed to decrease as the filter plugged. Filter plugging was arbitrarily defined to have occurred at a 50% reduction in flow from the design value. Table II is a summary of these results.

From the data in Table II, we can observe that increasing the stearic acid concentration by increasing the generation rate from 0.105 to 2.05 cm<sup>3</sup>/min in the absence of water spray successively reduced plugging times from 32.2 h to 4.87 h. Adding water spray at the higher particle flow rates (200 g/min

TABLE II  
SUMMARY OF IDEALIZED FILTER PLUGGING TESTS  
USING STEARIC ACID AND WATER SPRAY

Test	Stearic Acid Volumetric Flow Rate (cm <sup>3</sup> /min)	Water Mass Flow Rate (g/min)	Plugged Mass (kg)	Time to Plug (h)
17	0.0	100	3.447	27.0
18	0.0	200	7.729	9.52
19	0.0	400	6.996	5.27
4	0.105	0	0.415	32.2
7	0.105	100	6.481	32.9
6	0.105	200	8.060	5.787
5	0.105	400	6.583	4.93
1	0.241	0	0.401	20.7
10	0.241	100	6.179	31.5
9	0.241	200	6.941	4.53
8	0.241	400	6.336	4.13
2	0.941	0	0.550	13.4
13	0.941	100	3.796	6.22
12	0.941	200	5.429	6.23
11	0.941	400	5.450	3.90
3	2.05	0	0.454	4.87
16	2.05	100	4.251	5.97
15	2.05	200	5.345	6.05
14	2.05	400	6.449	3.00

and 400 g/min) resulted in faster plugging (about 3--6 h) with higher total mass loadings (about 5.5--8 kg) of water and stearic acid. In addition, dry stearic acid plugged the filters with significantly less mass loading (about 0.40--0.55 kg).

Figures 11 and 12 present the results of the eight filter tests conducted at the highest and lowest stearic acid mass generation rates, respectively. These curves can be fitted with polynomials of the form  $\Delta p/\Delta p_0 = f(m_p)$ , where  $f$  is a polynomial and includes the linear form of Eq. (1). In this way the data could be used in a computer code to estimate pressure drops during filter plugging under fire conditions.

Repetitive mass measurements at individual points during filter plugging showed that the working resolution of the mass balance/transducer combination was 2 to 3 g.

#### IV. FUTURE FILTER PLUGGING TESTS

A more complicated series of filter plugging tests will be conducted during 1982. This series will use the same weighing technique but also will use a special combustor designed by Battelle Pacific Northwest Laboratory to burn two materials, polystyrene (PS) and polymethylmethacrylate (PMMA), at high and low mass-burning (or smoke-generation) rates. (See Table I.) The mass-burning rates will be controlled by adjusting the inlet air supply rate. Each of these conditions will be repeated 3 times for a total of 12 tests. (The repetitions will allow us to assess the reproducibility of our test results.) Because PS and PMMA represent extremes of smoke-producing materials, we should be able to derive filter plugging coefficients that bracket those expected in nuclear fuel cycle facility fires. Additional experiments should be performed, including using typical fuel mixtures, adding heat and moisture to the flow, and using improved gas analysis and particle-size measuring instrumentation. Such tests should simulate and measure more complex and more realistic filter plugging conditions.

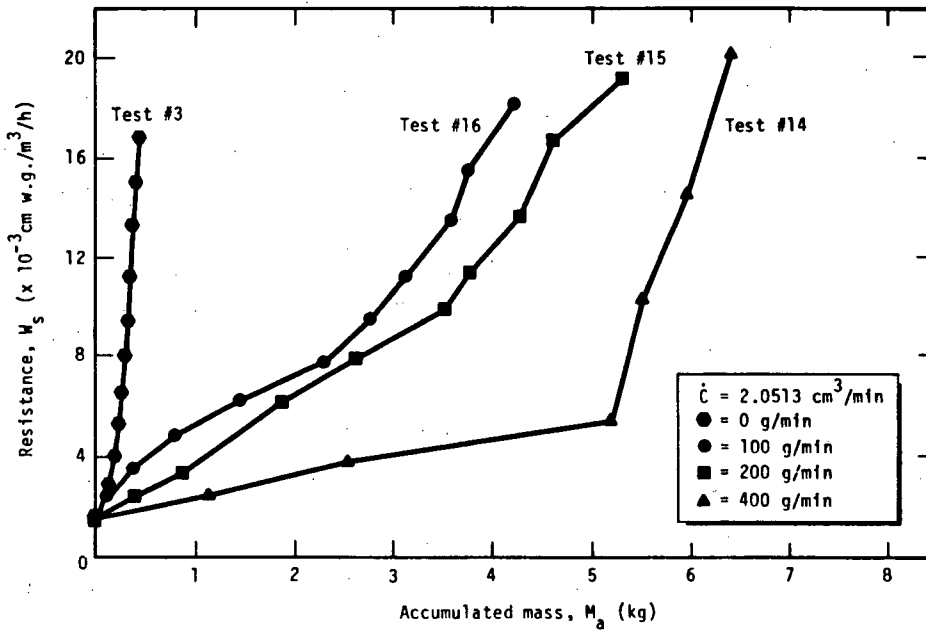


Fig. 11.  
Resistance—mass loading curves.

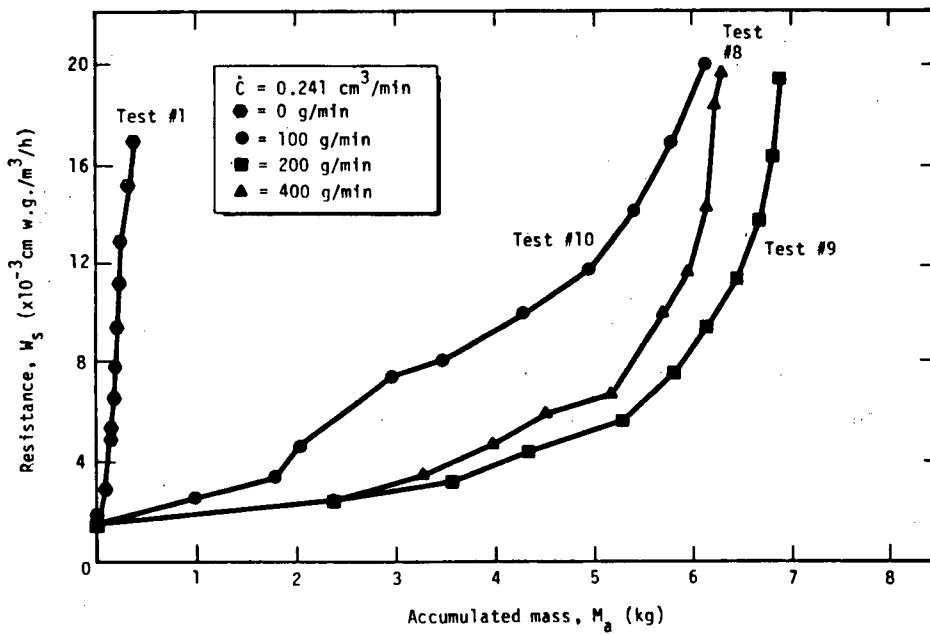


Fig. 12.  
Resistance—mass loading curves

## V. SUMMARY AND CONCLUSIONS

Los Alamos, in cooperation with NMSU, is conducting an experimental study in which HEPA filters are being subjected to simulated fire accident conditions. The purpose of this study is to obtain supportive data with which to improve the existing mathematical models of filter plugging under fire conditions or formulate new ones. Such models currently are being used in the Los Alamos nuclear fuel cycle facility accident analysis computer code FIRAC.

In this paper we described the Los Alamos/NMSU HEPA filter plugging test facility and presented some results of preliminary tests conducted in it. This filter plugging facility can supply much-needed experimental data to support filter plugging modeling and computer code development. We also outlined some recently accomplished idealized tests using stearic acid and some plans for ongoing ones using nonradioactive combustible materials found in fuel cycle facilities.

In summary, the idealized tests support the following conclusions.

- (1) The balance beam/force transducer weighing assembly is an acceptable weighing system for detecting HEPA filter mass accumulations with a resolution of 2 to 3 g.
- (2) These tests established that water vapor is an important variable in the loading of HEPA filters with a combustion aerosol. The filter lifetime is dependent on the amount of water vapor in the aerosol. Filter 14, loaded at the maximum average particle generation rate of  $2.0513 \text{ cm}^3/\text{min}$  and at the maximum water vapor addition rate of 400 g/min, had the shortest lifetime—3 h.
- (3) Water vapor loading creates a larger mass deposit on the filter at the fully plugged condition than the dry particulate loading. The filters loaded with water vapor had mass loadings greater than 3400 g, whereas the filters loaded with the dry aerosol had mass loadings less than 550 g.
- (4) Filters loaded with combined wet and dry aerosols have resistance/mass loading curves that lie between the curves of the pure water-loaded and pure particle-loaded filters.



## REFERENCES

1. W. S. Gregory, R. A. Martin, P. R. Smith, and D. E. Fenton, "Response of HEPA Filters to Simulated Accident Conditions," Proc. of the 17th DOE Nuclear Air Cleaning Conference, Denver, Colorado, August 2--5, 1982, DOE Conf-820833 (February 1983), Vol. II, pp. 1051-1066.
2. C. A. Burchsted, A. B. Fuller, J. E. Kahn, "Nuclear Air Cleaning Handbook," Oak Ridge National Laboratory ERDA report 76-21 (March 1976).
3. "Fuel Cycle Facility Accident Analysis Handbook," Los Alamos National Laboratory report LA-9180-M, NUREG/CR-2508, PNL-4149 in preparation.
4. R. W. Andrae, J. W. Bolstad, W. S. Gregory, F. R. Krause, R. A. Martin, and P. K. Tang, "FIRAC Users Manual - A Computer Code for Analysis of Fire-induced Flow and Material Transport Nuclear Facilities," Los Alamos National Laboratory report in preparation.
5. R. A. Martin, P. K. Tang, A. P. Harper, J. D. Novat, and W. S. Gregory, "Material Transport Analysis for Accident-induced Flow in Nuclear Facilities," Los Alamos National Laboratory report LA-9913-MS, NUREG/CR-3527 (September 1983).
6. W. Bergman, H. Hebard, R. Taylor, and B. Lum, "Electrostatic Filters Generated by Electric Fields," Lawrence Livermore Laboratory paper UCRL-81926 (July 1979), submitted to Second World Filtration Congress, London, September 18--20, 1979.
7. N. A. Fuchs, The Mechanics of Aerosols (Pergamon Press Ltd., Oxford, 1964).
8. C. N. Davies, Air Filtration (Academic Press, New York, 1973).
9. C. N. Davies, Ed., Aerosol Science (Academic Press, New York, 1966).
10. "Operation and Maintenance Manual for Royco Model 258 Smoke Generator, Stock No. 197-006," Hiac/Royco Instruments, Menlo Park, California (October 1981).
11. V. M. Faries, Design of Machine Elements (MacMillan Co., New York, 1965).
12. J. J. Dallman, "HEPA Filter Loading by Simulated Combustion Products," Masters Thesis submitted to Mechanical Engineering Department, New Mexico State University (1982).

DISTRIBUTION

	<u>Copies</u>
Nuclear Regulatory Commission, RI, Bethesda, Maryland	173
Technical Information Center, Oak Ridge, Tennessee	2
Los Alamos National Laboratory, Los Alamos, New Mexico	<u>50</u>
	225